J|A|C|S
ARTICLES
Published on Web 12/10/2003

The Rearrangements of Naphthylnitrenes: UV/Vis and IR Spectra of Azirines, Cyclic Ketenimines, and Cyclic Nitrile Ylides

Alexander Maltsev,[†] Thomas Bally,*[,†] Meng-Lin Tsao,[‡,||] Matthew S. Platz,*[,‡] Arvid Kuhn,[§] Michael Vosswinkel,[§] and Curt Wentrup*[,§]

Contribution from the Department of Chemistry, University of Fribourg, CH-1700 Fribourg, Switzerland, Department of Chemistry, The Ohio State University, Columbus, Ohio 43210, and Chemistry Department, School of Molecular and Microbial Sciences, The University of Queensland, Brisbane, Qld 4072, Australia

Received September 11, 2003; E-mail: thomas.bally@unifr.ch

Abstract: Ar matrix photolysis of 1- and 2-naphthyl azides **3** and **4** at 313 nm initially affords the singlet naphthyl nitrenes, ^{1}**1** and ^{1}**2**. Relaxation to the corresponding lower energy, persistent triplet nitrenes ^{3}**1** and ^{3}**2** competes with cyclization to the azirines **15** and **18**, which can also be formed photochemically from the triplet nitrenes. On prolonged irradiation, the azirines can be converted to the seven-membered cyclic ketenimines **10** and **13**, respectively, as described earlier by Dunkin and Thomson. However, instead of the *o*-quinoid ketenimines **16** and **19**, which are the expected primary ring-opening products of azirines **15** and **18**, respectively, we observed their novel bond-shift isomers **17** and **20**, which may be formally regarded as cyclic nitrile ylides. The existence of such ylidic heterocumulenes has been predicted previously, but this work provides the first experimental observation of such species. The factors which are responsible for the special stability of the ylidic species **17** and **20** are discussed.

Introduction

The 1- and 2-naphthylnitrenes (**1** and **2**) can be generated by direct[1−3] or sensitized[4] photolysis, or by pyrolysis from the corresponding azides **3** or **4**,[2,5] respectively (Scheme 1). An alternate source of **1** and **2** are triazoles **5** or **6**, respectively, which can be decomposed by flash vacuum pyrolysis.[6] In the latter reactions, the naphthyl nitrenes are formed via a carbene−nitrene rearrangement[7−10] from the quinoyl (**7**) or isoquinoyl (**8**) carbenes, respectively. These transformations are presumed to involve the intermediate azirines **9**, **11**, **12**, and **14** and the didehydroazepines **10** and **13**, respectively. None of these intermediates are, however, detectable under the conditions of thermal equilibration of carbene **7** with the (more stable[7,8,11,12]) nitrene **1**, or **8** with **2**.

On the other hand, Dunkin and Thomson had found earlier that irradiation of the naphthyl azides **3** and **4** led to the occurrence of IR bands at 1710−1740 cm^{-1}, which they interpreted as being indicative of bicyclic azirines such as **11** and/or **15** (from **1**), and **14** and/or **18** (from **2**). On further irradiation, these bands gave way to new absorptions in the 1910−1930 cm^{-1} region which were assigned to the cyclic ketenimines **10** or **16** (from **1**), and **13** and/or **19** (from **2**).[13] Thus, a whole range of interesting reactive intermediates can potentially be accessed from the naphthylnitrenes **1** and **2** or from the triazoles **5** and **6**.

Moreover, recent computational work has demonstrated the possibility that *o*-quinoid cyclic ketenimines such as **16** or **19** may exist independently in the form of (aromatic) ylidic azaallenes **17** or **20**, respectively.[14] We now report a comprehensive investigation of the fate of the two naphthylnitrenes on photolysis in Ar matrices as well as a quantum chemical study of the potential energy surfaces on which the possible rearrangements take place.

Experimental and Theoretical Methods

The naphthyl azides **3** and **4** were synthesized according to literature procedures.[15] After evaporating a few milliliters of a concentrated pentane solution of the precursors to dryness in a U-tube, the tube was attached to the inlet system of a cryostat. After evacuation, the compounds were entrained by a stream of Ar and deposited on a CsI window kept at ca. 20 K while the U-tube was kept at −17 °C (**3**) or −5 °C (**4**). In this way, matrices containing suitable concentrations of **3** or **4** could be generated reproducibly. The samples were exposed to

[†] University of Fribourg.
[‡] The Ohio State University.
[§] The University of Queensland.
[||] Current address: The Scripps Research Institute, La Jolla, CA 92037.

(1) Reiser, A.; Frazer, V. *Nature (London)* **1965**, *208*, 682.
(2) Hilton, S. E.; Scriven, E. F.; Suschitzky, H. *J. Chem. Soc., Chem. Commun.* **1974**, 853.
(3) Schrock, A. K.; Schuster, G. B. *J. Am. Chem. Soc.* **1984**, *106*, 5234.
(4) Leyshon, L. J.; Reiser, A. *J. Chem. Soc., Faraday Trans. 2* **1972**, *68*, 1918.
(5) Boshev, G.; Dyall, L. K.; Sadler, P. R. *Aust. J. Chem.* **1972**, *25*, 599.
(6) Kuzaj, M.; Lüerssen, H.; Wentrup, C. *Angew. Chem., Int. Ed. Engl.* **1986**, *25*, 480.
(7) Wentrup, C. *Top. Curr. Chem.* **1976**, *62*, 173.
(8) Platz, M. S. *Acc. Chem. Res.* **1995**, *28*, 487.
(9) Karney, W. L.; Borden, W. T. *Adv. Carbene Chem.* **2001**, *3*, 205.
(10) Gritsan, N.; Platz, M. *Adv. Carbene Chem.* **2001**, *3*, 255.
(11) Wentrup, C. *Reactive Molecules*; Wiley-Interscience: New York, 1985.
(12) Kemnitz, C. R.; Karney, W. L.; Borden, W. T. *J. Am. Chem. Soc.* **1998**, *120*, 3499.
(13) Dunkin, I. R.; Thomson, P. C. P. *J. Chem. Soc., Chem. Commun.* **1980**, 499.
(14) Kuhn, A.; Vosswinkel, M.; Wentrup, C. *J. Org. Chem.* **2002**, *67*, 9023.
(15) Forster, M. O.; Fierz, H. E. *J. Chem. Soc.* **1907**, 1942.

Scheme 1. Scheme of Compounds Discussed in the Present Study

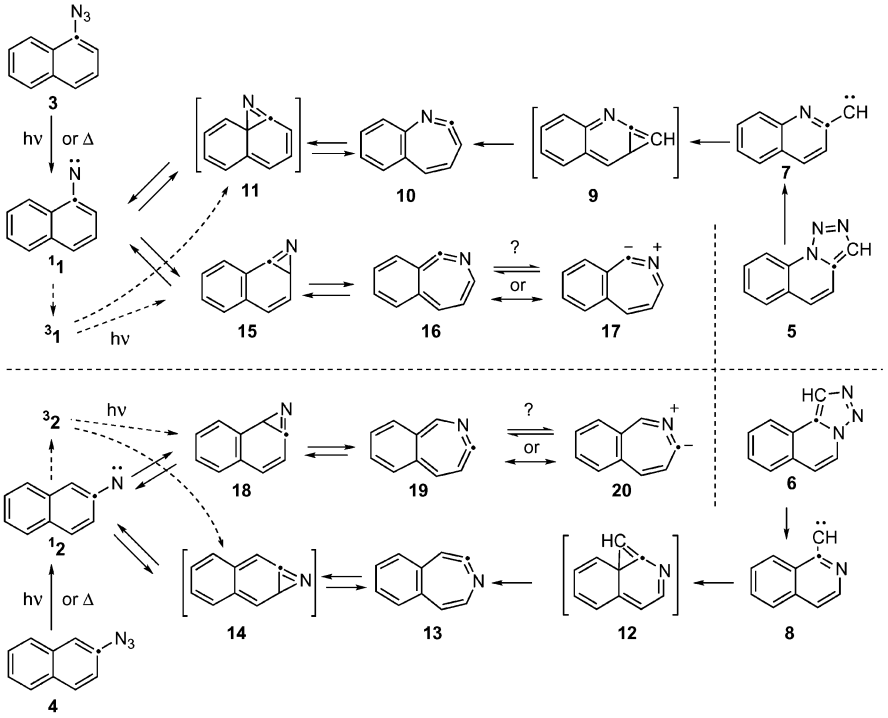

radiation produced either from a 150 W medium-pressure Hg lamp (313 or 365 nm) or from a 1 kW Hg/Xe lamp (for other wavelengths), using combinations of interference and/or long pass filters. For 254 nm irradiation, a 20 W low-pressure Hg lamp was used. FT-IR spectra were recorded on a Michelson interferometer whose sample chamber was evacuated to 0.2 Torr.

All calculations, except those for the singlet naphthylnitrenes and the transition states for their ring closure to azirines, were carried out using the B3LYP combination of exchange and correlation functionals[16,17] (as implemented in the Gaussian 98 suite of programs[18]), which has amply proven to be adequate for predicting structures and energies of species similar to those considered in the present study.[12,14,19−29] Geometry optimizations and frequency calculations were done with the 6-31G* basis set, whereas the larger 6-311+G(2d,p) basis set was used to calculate relative energies which were then corrected by zero-point energies from the above frequency calculations. Some key intermediates were reoptimized at the B3LYP/6-31+G* level of theory, which usually had no significant effect on the stuctures or relative energies but can cause significant shifts to lower wavenumbers in the infrared spectra of zwitterionic compounds.[14,27,28,30] For comparison with experimental IR spectra, vibrational frequencies were scaled by a factor of 0.97 throughout.[31]

Because singlet nitrenes have an open-shell biradicaloid electronic structure, their proper description requires two determinants, which makes it impossible to use standard DFT methods.[32] Thus, the naphthylnitrenes, the transition states for their ring closure to azirines, and the azirines themselves were optimized and characterized as stationary points of the proper kind at the CASSCF(12,12)/ 6-31G* level, where the active space included 11 π and π^* MOs of the naphthalene ring and the in-plane 2p(σ) AO of the nitrogen atom. Relative energies of singlet and triplet nitrenes were then calculated at the CASPT2 level and corrected for CASSCF zero-point energies. Using the triplet naphthylnitrenes, whose energies can be computed straightforwardly by DFT, as a common basis, this approach made it possible to put all of the species on a common scale.[33]

It was found that the diradicaloid character of the singlet nitrenes decreases steadily along the pathway for cyclization to azirines (at the corresponding transition states, the natural orbital occupation number of the "HOMO" had already dropped to 0.26−0.30). Therefore, we attempted the calculation of these transition states also by the DFT method, which has in other cases proven to be surprisingly robust with regard to treating biradicaloid species.[34,35] However, as was found in a

(16) Becke, A. D. *J. Chem. Phys.* **1993**, *98*, 5648.
(17) Lee, C.; Yang, W.; Parr, R. G. *Phys. Rev. B* **1988**, *37*, 785.
(18) Frisch, M. J.; Trucks, G. W.; Schlegel, H. B.; Scuseria, G. E.; Robb, M. A.; Cheeseman, J. R.; Zakrzewski, V. G.; Montgomery, J. A.; Stratmann, R. E.; Burant, J. C.; Dapprich, S.; Millam, J. M.; Daniels, A. D.; Kudin, K. N.; Strain, M. C.; Farkas, O.; Tomasi, J.; Barone, V.; Cossi, M.; Cammi, R.; Mennucci, B.; Pommelli, C.; Adamo, C.; Clifford, S.; Ochterski, J.; Petersson, G. A.; Ayala, P. Y.; Cui, Q.; Morokuma, K.; Malick, D. K.; Rabuck, A. D.; Raghavachari, K.; Foresman, J. B.; Cioslowski, J.; Ortiz, J. V.; Stefanov, B. B.; Liu, G.; Liashenko, A.; Piskorz, P.; Komaromi, I.; Gomperts, R.; Martin, R. L.; Fox, D. J.; Keith, T.; Al-Laham, M. A.; Peng, C. Y.; Nanayakkara, A.; Challacombe, M.; Gill, P. M. W.; Johnson, B. G.; Chen, W.; Wong, M. W.; Andres, J. L.; Gonzales, C.; Head-Gordon, M.; Repogle, E. S.; Pople, J. A.: *Gaussian 98*, revision A1; Gaussian, Inc.: Pittsburgh, PA, 1998.
(19) Evans, R. A.; Wong, M. W.; Wentrup, C. *J. Am. Chem. Soc.* **1996**, *118*, 4009.
(20) Matzinger, S.; Bally, T.; Patterson, E. V.; McMahon, R. J. *J. Am. Chem. Soc.* **1996**, *118*, 1535.
(21) Wong, M. W.; Wentrup, C. *J. Org. Chem.* **1996**, *61*, 7022.
(22) Karney, W. L.; Borden, W. T. *J. Am. Chem. Soc.* **1997**, *119*, 1378.
(23) Matzinger, S.; Bally, T. *J. Phys. Chem. A* **2000**, *104*, 3544.
(24) Bonvallet, P. A.; McMahon, R. J. *J. Am. Chem. Soc.* **2000**, *122*, 9332.
(25) Bonvallet, P. A.; Todd, E. M.; Kim, Y. S.; McMahon, R. J. *J. Org. Chem.* **2002**, *67*, 9031.
(26) Geise, C. M.; Hadad, C. M. *J. Org. Chem.* **2002**, *67*, 2532.
(27) Addicott, C.; Reisinger, A.; Wentrup, C. *J. Org. Chem.* **2003**, *68*, 1470.
(28) Addicott, C.; Wong, M. W.; Wentrup, C. *J. Org. Chem.* **2002**, *67*, 8538.
(29) Pritchina, E. A.; Gritsan, N. P.; Maltsev, A.; Bally, T.; Autrey, T.; Liu, Y.; Wang, Y.; Toscano, J. *Phys. Chem. Chem. Phys.* **2003**, *5*, 1010.
(30) Plüg, C.; Wallfisch, B.; Andersen, H. G.; Bernhardt, P. V.; Baker, L.-J.; Clark, G. R.; Wong, M. W.; Wentrup, C. *J. Chem. Soc., Perkin Trans. 2* **2000**, 2096.
(31) In the literature, slightly smaller scaling factors of 0.9614 (Scott, A. P.; Radom, L. *J. Phys. Chem.* **1996**, *100*, 16502) and 0.9613 (Wong, M. W. *Chem. Phys. Lett.* **1996**, *256*, 391) have been proposed. The factor of 0.97 has often given better agreement with experiment in our work on reactive intermediates, which were not part of the "training sets" used in the above studies (cf. e.g.: Pritchina, E. A.; Gritsan, N. P.; Maltsev, A.; Bally, T.; Autrey, T.; Liu, Y.; Wang, Y.; Toscano, J. P. *Phys. Chem. Chem. Phys.* **2003**, *5*, 1010 or Bednarek, P.; Zhu, Z.; Bally, T.; Filipiak, T.; Marcinek, A.; Gebicki, J. *J. Am. Chem. Soc.* **2001**, *123*, 2377).
(32) Tsao, M.-L.; Gritsan, N.; James, T. R.; Platz, M. S.; Hrovat, D. A.; Borden, W. T. *J. Am. Chem. Soc.* **2003**, *125*, 9343.
(33) Tsao, M.-L.; Platz, M. S. *J. Am. Chem. Soc.* **2003**, *125*, 12014.

recent study on *o*-biphenylnitrenes,[32] the (restricted) B3LYP wave function turns out to be unstable toward UHF symmetry breaking at these geometries, but reoptimization of the transition states by the UB3LYP method (whereby the expectation value of S^2 increased to 0.25−0.3) led to geometries that did not deviate much from those obtained by CASSCF calculations and to activation energies in good accord with those found by CASPT2/CASSCF.[32]

Excited state calculations were carried out by the TD-DFT procedure,[36] using the B3LYP functional with the 6-31G* basis set as implemented in the Gaussian programs.[37] In the case of the naphthylnitrenes, we also carried out CASSCF/CASPT2 calculations[38] with the ANO/S basis set[39] (at the CASSCF geometries, see above). To eliminate intruder states in the CASPT2 runs for all excited states under consideration, a level shift of 0.3 h had to be applied.[40] Under this condition, the weight of the zero-order CASSCF wave function in the PT2 expansion was between 0.7 and 0.72 for all states. All CASSCF/CASPT2 calculations were performed with the Molcas program.[41]

In compounds **30′** and **31′**, nuclear-independent chemical shift (NICS) values (which constitute a measure of aromaticity or antiaromaticity)[42] were computed as the negative isotropic value of the nuclear magnetic shielding tensor of a ghost atom placed at the barycenter of the molecule and computed by the gauge-independent atomic orbital (GIAO) method[43] within the B3LYP/ 6-31G* model. The same model was also used to compute atomic charges by the ChelpG scheme (charges from electrostatic potentials on a grid of points)[44] used in the analysis of **30′** and **31′**. The above calculations were also carried out with the Gaussian 98 suite of programs.[18]

Results and Discussion

1. Matrix Isolation Spectroscopy. Usually, 254 nm light is used to deazotate matrix isolated aryl azides. However, we found that at this wavelength complete decomposition of the naphthyl azides (which was necessary to follow the subsequent rearrangements) led to a multitude of products that could not be easily distinguished. In contrast, 313 nm irradiation, which also allowed complete decomposition of **3** and **4** in ca. 20 min, led to much "cleaner" samples.

1-Naphthyl Azide. Irradiation of **3** at 313 nm for 20 min led to the UV−vis spectrum shown in Figure 1a, which clearly shows the sharp bands of triplet 1-naphthylnitrene, ^{3}**1**, next to a weak broad band that extends from 350 to 600 nm (cf. expanded inset in Figure 1). The spectrum is similar to that obtained by Reiser and Frazer almost 40 years ago in an organic glass at 77 K.[1] Because the new absorption extends beyond that of ^{3}**1**, it can be bleached completely in 15 min by irradiation at >545 nm, that is, in a region where ^{3}**1** does not absorb. For this reason, the yield of nitrene increases only very slightly (see 530 nm band, spectrum 1b), but an absorption in the 280−360 nm region grows more substantially. The latter band will be assigned to the azirine **15** below. Subsequent irradiation for 30 min at >515 nm then bleaches ^{3}**1** and leaves a spectrum with no structured bands above 300 nm, but an increased absorption below 300 nm (spectrum 1c).

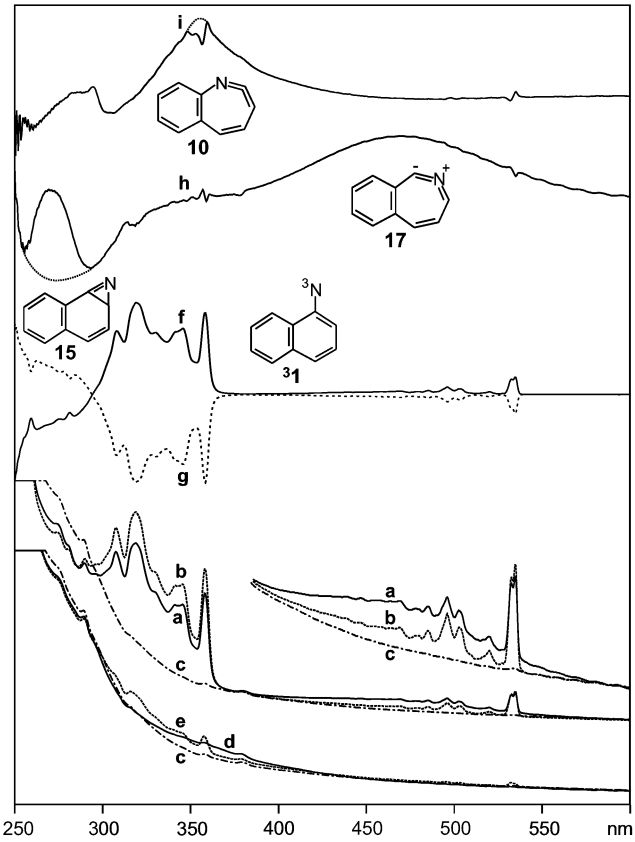

Figure 1. UV/vis spectra obtained after (a) decomposition of 1-naphthyl azide **3** at 313 nm; (b) subsequent irradiation at >545 nm; (c) bleaching of nitrene **1** at >515 nm; (d) after regeneration of **1** at 313 nm and bleaching at >515 nm of the species absorbing above 400 nm; (e) after photolysis at 365 nm (until a photostationary equilibrium is reached). (f) Difference spectrum for the formation of **1**; (g) difference spectrum for the bleaching of **1**; (h) inverted difference spectrum for the bleaching of **17** (corrected for the absorptions of **1**); (i) inverted difference spectrum for the bleaching of ketenimine **10** (corrected for the absorptions of **1**).

Although no azide is left in the sample at this stage, returning to 313 nm irradiation restores a spectrum very similar to trace 1a, thus suggesting that the nitrene and the azirine exist in a photochemically reversible equilibrium. However, after both the nitrene and the broad 350−600 nm band are bleached by >515 nm irradiation, spectrum 1d is left, which, if superimposed onto spectrum 1c, appears to show an enhanced absorption at 330−430 nm. Indeed, photolysis of this sample for 30 min at 365 nm leads to a decrease in this region which is partially offset by the restoration of absorptions of ^{3}**1** (spectrum 1e).

From the above spectra, one can generate, by suitable formation of differences, the UV/vis spectra of four compounds as shown in the upper part of Figure 1. Spectrum 1f shows the reformation of the nitrene by 313 nm irradiation (at a stage where no azide was left in the matrix), and 1g shows its subsequent bleaching at >515 nm (after bleaching the broad

(34) Hrovat, D. A.; Duncan, J. A.; Borden, W. T. *J. Am. Chem. Soc.* **1999**, *121*, 169.
(35) Johnson, W. T. G.; Sullivan, M. B.; Cramer, C. J. *Int. J. Quantum Chem.* **2001**, *85*, 492.
(36) Casida, M. E. In *Recent Advances in Density Functional Methods, part I*; Chong, D. P., Ed.; World Scientific: Singapore, 1995; p 155.
(37) Stratmann, R. E.; Scuseria, G. E.; Frisch, M. J. *J. Chem. Phys.* **1998**, *109*, 8218.
(38) Andersson, K.; Roos, B. O. *Modern Electronic Structure Theory*; World Scientific Publ. Co.: Singapore, 1995; Vol. Part 1, Vol. 2; p 55.
(39) Pierloot, K.; Dumez, B.; Widmark, P.-O.; Roos, B. O. *Theor. Chim. Acta* **1995**, *90*, 87.
(40) Roos, B. O.; Andersson, K.; Fülscher, M. P.; Serrano-Andrés, L.; Pierloot, K.; Merchan, M.; Molina, V. *J. Mol. Struct. (THEOCHEM)* **1996**, *388*, 257.
(41) Andersson, K.; Barysz, M.; Bernhardsson, A.; Blomberg, M. R. A.; Cooper, D. L.; Fleig, T.; Fülscher, M. P.; Graaf, C. d.; Hess, B. A.; Karlström, G.; Lindh, R.; Malmqvist, P.-Å.; Neogrády, P.; Olsen, J.; Roos, B. O.; Sadlej, A. J.; Schütz, M.; Schimmelpfennig, B.; Seijo, L.; Serrano-Andrés, L.; Siegbahn, P. E. M.; Stålring, J.; Thorsteinsson, T.; Veryazov, V.; Widmark, P.-O. MOLCAS, Version 5; University of Lund: Sweden, 2000.
(42) Schleyer, P. v. R.; Maerker, C.; Dransfeld, A.; Jiao, H.; Hommes, N. J. R. E. *J. Am. Chem. Soc.* **1996**, *118*, 6317.
(43) Weeny, R. M. *Phys. Rev.* **1962**, *126*, 1028.
(44) Breneman, C. M.; Wiberg, K. *J. Comput. Chem.* **1990**, *11*, 361.

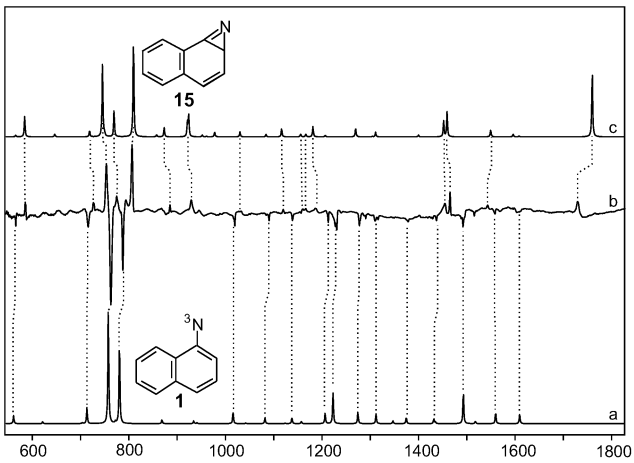

Figure 2. (a) B3LYP/6-31G* calculated IR spectrumof nitrene **1** (scaling factor 0.97); (b) difference spectrum for bleaching of nitrene **1** on >515 nm irradiation; (c) B3LYP/6-31G* calculated IR spectrum of azirine **15** (scaling factor 0.97).

350−600 nm band by >545 nm irradiation). The two spectra are almost exact mirror images, and they show that the processes of formation and bleaching of ^{3}**1** are accompanied by a concomitant decrease or increase, respectively, of a species that absorbs below 300 nm (and, apparently, also to some extent above 300 nm because it can be bleached at 313 nm). This absorption is assigned to azirine **15**. Trace 1h is equal to the difference spectrum 1a−1b (where the absorptions due to ^{3}**1** were eliminated by subtracting a scaled spectrum 1f). It thus represents the spectrum of the species with the weak 350−600 nm band which is found to peak at about 470 nm and will be assigned to ylide **17**. It appears to be accompanied by a sharper band peaking at ca. 265 nm. This UV band is superimposed on a decreasing absorption that sets in at ca. 320 nm and belongs presumably to the same species which gives rise to the UV part of Figure 1f/g. Finally, the spectrum of the compound which is responsible for the broad 300−400 nm absorption (Figure 1i) is obtained from the difference spectrum 1d−1e, corrected again for the absorptions of ^{3}**1**. This spectrum shows a band with a maximum at ca. 350 nm (the sharp features at the top of this band are due to incomplete subtraction of the spectrum of ^{3}**1**), and perhaps another one at ca. 280 nm. It will be assigned to the cyclic ketenimine **10**.

The transformations described above were also followed by IR spectroscopy. We first discuss the IR difference spectrum which corresponds to spectrum 1c−1b, that is, the photolysis of the triplet nitrene (Figure 2b). The negative peaks in this trace correlate very well with those in the calculated spectrum of ^{3}**1** shown in Figure 2a, thus confirming their assignment to the nitrene. Among the two azirines which may conceivably be formed as primary photoproducts of ^{3}**1** (cf. Scheme 1), the calculated IR spectrum of azirine **15** (Figure 2c) shows a much better correlation with the positive peaks in the experimental spectrum than does the calculated spectrum of azirine **11** (which in fact is not a minimum on the B3LYP/6-31G* potential energy surface, see below).[45] Moreover, **11** would be expected to show absorptions extending beyond 350 nm in the UV due to the *o*-quinoid nature of its π-system, in contrast to **15** which is formally a styrene derivative.

The experimental IR spectrum in Figure 3a (negative peaks) corresponds to the optical spectrum in Figure 1h. Because azirine

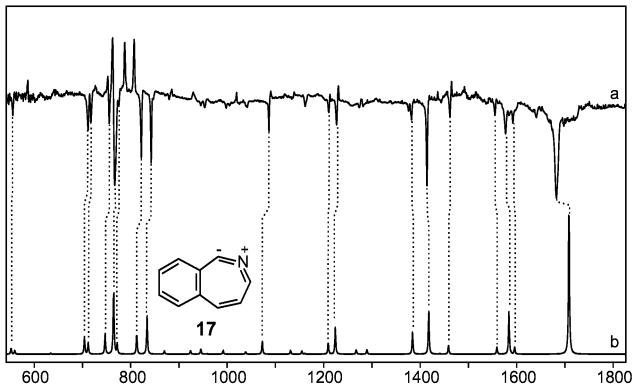

Figure 3. (a) Difference spectrum for bleaching of ylide **17** on >545 nm irradiation; (b) B3LYP/6-31G* calculated IR spectrum of ylide **17** (scaling factor 0.97).

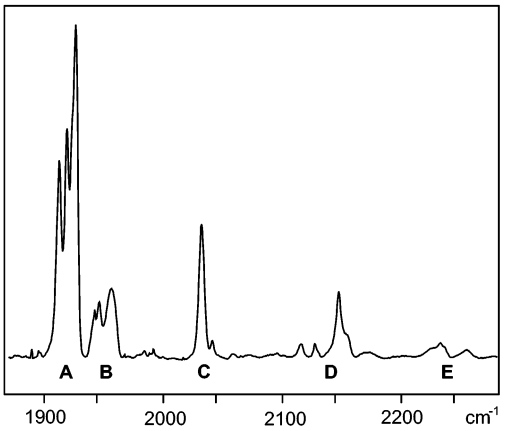

Figure 4. IR spectrum obtained after several cycles of 313 and >515 nm irradiation.

15 appears to be the primary photoproduct of nitrene ^{3}**1**, one would have assumed that ketenimine **16** is the secondary photoproduct. However, the IR spectrum calculated for this species (see Supporting Information) shows a very strong band at 1812 cm^{-1} (1800 cm^{-1} by B3LYP/6-31+G*) which is in very poor accord with the 1683 cm^{-1} band in the experimental spectrum (Figure 3a). Also, the remainder of the calculated spectrum of **16** shows no evident relation to the pattern of negative peaks in Figure 3a. In contrast, the calculated IR spectrum of the novel cyclic nitrile ylide **17** (Figure 3b) is in excellent agreement with the experimental one (Figure 3a), barring the intense 1709 cm^{-1} band, which is predicted at slightly too high of an energy.

In the course of the different irradiations described above, more peaks began to accumulate in the region of 1900−2300 cm^{-1}. An example of an (absolute) spectrum, obtained after several cycles of 313 nm formations and >545/>515 nm bleachings, is shown in Figure 4. It shows groups of peaks that belong to at least five different types of species labeled **A**−**E**. Although species **A** and **B** can be partially bleached on >375

(45) The only other such azirines (7-aza-2,4,6-bicyclo[4.1.0]heptatrienes) whose IR spectra have been reported to date are those which result from the cyclization of 2,5-difluoro- or perfluorophenylnitrene (Morawietz, J.; Sander, W. *J. Org. Chem.* **1996**, *61*, 4351) or of 3-isoquinoylnitrene (Wentrup, C. In *Azides and Nitrenes*; Scriven, E. F. V., Ed.; Academic Press: Orlando, FL, 1984; p 421). These azirines show C=N streching vibrations that vary between 1664 and 1725 cm^{-1}, and they are all lower than the 1731 cm^{-1} observed for **15**. However, due to the different mode mixings which prevail in these different compounds, the positions of these IR bands cannot be directly compared.

Scheme 2. Possible Ring-Opening Pathways and Products of **1** and **10**

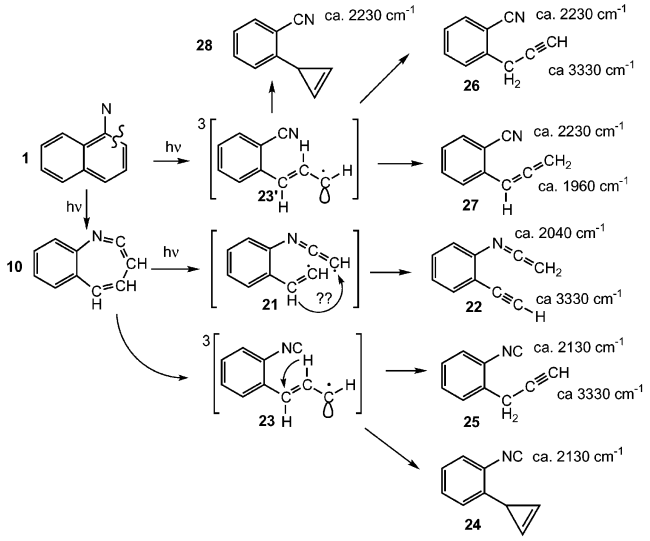

nm irradiation, and **C** disappears gradually on prolonged 313 nm photolysis, all efforts to extract full IR difference spectra for comparison to calculated spectra of different candidate compounds (see below) failed. Only in the case of **A** did a careful comparison of different spectra reveal some peaks which correlate well with those calculated for the ketenimine **10** (cf. spectrum S2 in the Supporting Information), which was first observed by Dunkin and Thomson in their earlier exploratory experiments.[13] This species shows a typical band for a cyclic allenic ketenimine at ca. 1920 cm^{-1}, split into several components by site effects, as is not unusual for such types of vibrations.

In the absence of more definitive information, we can only speculate about the identity of species **B**−**E**. The band of **C** at 2040 cm^{-1} is reminiscent of those found for open-chain ketenimines, and one could surmise that such a species (**22**) may be formed by ring-opening of the cyclic ketenimine **10**. However, the formation of **22** requires a 1,6 H shift in the primary biradical, **21**, and this leads to a terminal C−C triple bond which should distinguish itself by a noticeable C−H stretching vibration at ca. 3330 cm^{-1}. The experimental spectrum shows, however, no trace of such a band.

Species **D** could possibly be an isocyanide (ν typically around 2130−2150 cm^{-1}). Again, it is conceivable that such a species might form by ring-opening of **10**. However, because we see no C(sp)−H stretching vibrations, the primarily formed vinylcarbene **23** would have to undergo cyclization to a cyclopropene, so that the resulting species would be **24**, rather than alkyne **25**. The multiple bands observed in the 2110−2150 cm^{-1} region could be due to different conformers of **24**, but we have to refrain from any definitive assignment due to lack of spectral information. Finally, the bands at 2210−2270 cm^{-1} would appear to belong to a nitrile. Scheme 2 sketches possible pathways leading to nitriles. Again, the absence of a band around 3330 cm^{-1} (terminal acetylene) excludes **26**, and the fact that the band at 1960 cm^{-1} can be bleached without affecting the bands of D excludes the allene **27**, so we are once more left with phenylcyclopropene **28** as a tentative candidate.

In sum, all that can be concluded from the presence of the IR bands shown in Figure 4 is that some ring-opening reactions must occur on prolonged irradiation of **1** and/or its rearrangement products. These transformations can be carried to completion because eventually we are left with an IR spectrum that shows no traces of ^{3}**1**, **15**, or **17**; that is, everything has been converted to ketenimine **10** and ring-opening products which are all quite photostable.

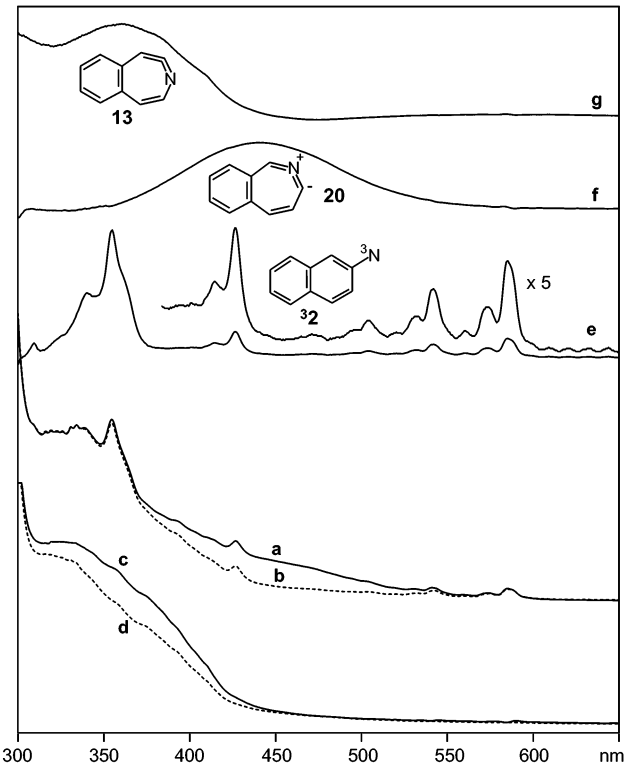

Figure 5. UV/vis spectra obtained after (a) decomposition of 2-naphthyl azide **4** at 313 nm; (b) subsequent irradiation at 470 nm; (c) bleaching of nitrene **2** at >515 nm; (d) after photolysis at 365 nm (until a photostationary equilibrium is reached). (e) Inverted difference spectrum for the bleaching of **4**; (f) inverted difference spectrum for the bleaching of **20**; (g) inverted difference spectrum for the bleaching of ketenimine **13** (corrected for the absorptions of **1**).

2-Naphthyl Azide. 2-Naphthyl azide **4** was also readily decomposed by 313 nm photolysis, which gave rise to the spectrum shown in Figure 5a. This spectrum contains again, next to the peaks of triplet 2-naphthylnitrene, ^{3}**2**, a broad band extending from 350 to 550 nm, but unlike the case for 1-naphthylnitrene, this absorption does not extend beyond the longest wavelength peak of ^{3}**2**. Therefore, irradiation at >545 nm led to concomitant bleaching of ^{3}**2** and of the broad band, but we found that the species responsible for that absorption undergoes at least partial selective bleaching on irradiation through a 470 nm interference filter, that is, at a wavelength where the absorptions of ^{3}**2** are minimal (spectrum 5b). Unfortunately, on longer irradiation at this wavelength, ^{3}**2** is also bleached, so that the sample could not be completely depleted of the species which gives rise to the broad band before photolyzing nitrene **2** by subsequent >545 nm photolysis, giving spectrum 5c. This spectrum shows a broad, probably composite band between 300 and 450 nm which can be partially bleached by further irradiation at 365 nm (spectrum 5d).

By forming suitable differences, three distinct spectra can be extracted from those shown in Figure 5a−d, that is, that of triplet 2-naphthylnitrene, ^{3}**2** (trace e), that of the species with the broad band which in this case peaks at 445 nm (trace f),

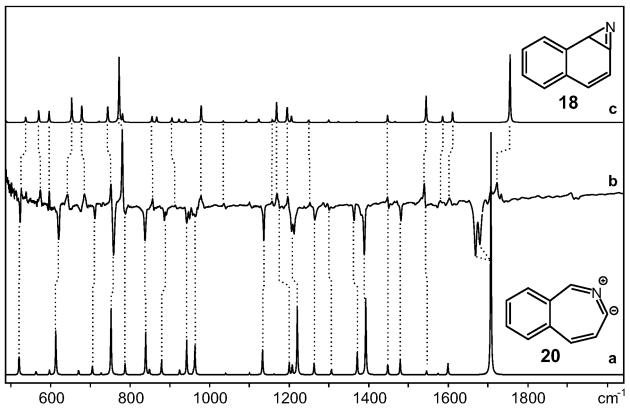

Figure 6. (a) B3LYP/6-31G* calculated IR spectrum for ylide **20**; (b) difference spectrum for conversion of ylide **20** into azirine **18** on 470 nm irradiation; (c) B3LYP/6-31G* calculated IR spectrum of azirine **18** (all calculated frequencies are scaled by 0.97).

which is assigned to the ylide **20** (see below), and finally that with the broad UV band (trace g) which we believe is due to ketenimine **13** (see below).

The same transformations were also studied by IR spectroscopy. Thus, Figure 6b shows a difference IR spectrum for the bleaching of the species with the broad 350−550 nm absorption (cf. spectrum 5f) at 470 nm. The most prominent IR transition for this species occurs in the form of a twin peak centered around 1680 cm^{-1}. Although this is not very far from the strongest IR peak predicted for azirine **18**, the rest of the spectrum shows so little resemblance to that calculated for **18** (trace 6c) that this assignment cannot be maintained. Instead, we found that the spectrum calculated for the ylidic heterocumulene **20** (trace 6a) shows near perfect agreement with the pattern of negative peaks in the experimental spectrum. The occurrence of two bands instead of one for the azaallene stretching vibration may be due to a pronounced site effect or perhaps to a Fermi resonance. This assignment being confirmed, azirine **18** was an evident candidate for the species which is formed on bleaching of **20**. Indeed, the pattern of positive peaks in the difference spectrum 6b shows very good agreement with the calculated spectrum of **18** (trace 6c).

Pinning down the IR spectrum of ^{3}**2** proved to be more difficult, because we could only obtain good IR spectra for the concomitant bleaching of ^{3}**2** and **20**. However, with the help of the difference spectrum for the bleaching of **20** alone (Figure 7a, copied from Figure 6b), the peaks due to nitrene ^{3}**2** which disappear on >590 nm irradiation could be discerned and correlated with the calculated spectrum for this species (trace 7c). Finally, it proved possible in the present 2-naphthyl case to assign also the IR spectrum of the aromatic ketenimine, **13**, as it is formed on 313 nm irradiation of a sample containing nitrene ^{3}**2**, azirine **18**, and ylide **20** (see Figure 8a). Again, the correspondence between the pattern of positive IR peaks and the calculated spectrum of **13** is very gratifying.

2. Calculations. 2.1. Potential Energy Surfaces. Schemes 3 and 4 show the relevant stationary points on the potential energy surfaces of the naphthylnitrenes. As outlined in Scheme 1, cyclization of ^{1}**1** and ^{1}**2** can lead to four isomeric azirines. We found, however, that not all of these represent (meta)stable intermediates. The bridgehead azirine **11** even turned out to be a transition state for the conversion of ^{1}**1** to ketenimine **10** at

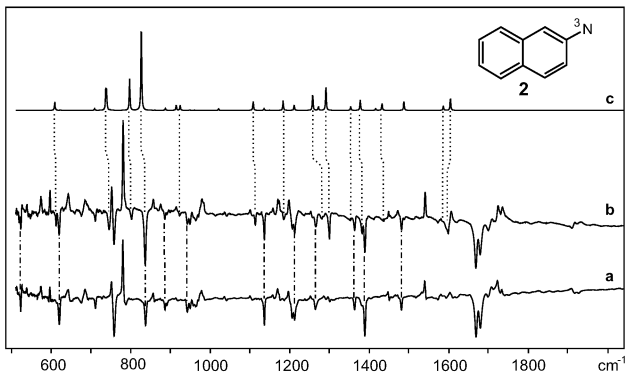

Figure 7. (a) Bleaching of ylide **20** on 470 nm irradiation (no nitrene **2** is bleached); (b) bleaching of nitrene **2** plus ylide **20** on >590 nm irradiation; (c) B3LYP/6-31G* calculated IR spectrum of nitrene **2** (scaled by 0.97).

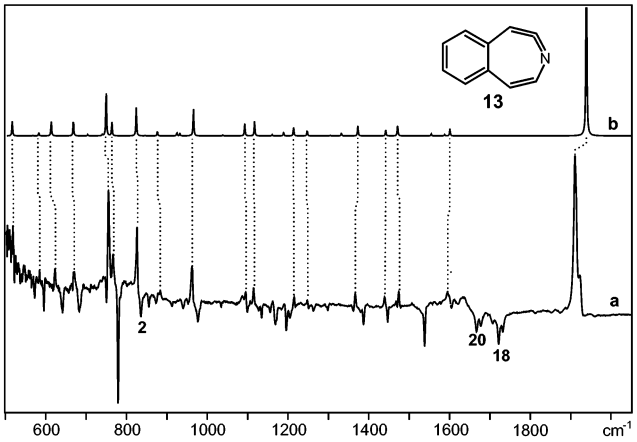

Figure 8. (a) Difference spectrum for formation of ketenimine **13** by irradiation of a matrix containing azirine **18**, ylide **20**, and nitrene **2** at 313 nm; (b) B3LYP/6-31G* calculated IR spectrum of ketenimine **13**.

the (U)B3LYP level. Although reoptimization at the CASSCF-(12,12) level revealed a (presumably very shallow) potential energy minimum for **11**, we did not attempt to locate the transition states on either side of **11** because the likelihood of verifying the exact nature of this fleeting species by experiment is very remote.

The *o*-quinoid azirine **14** which lies ca. 15 kcal/mol above its aromatic relative, **18**, corresponds to a shallow minimum on the B3LYP potential energy surface, but it is barely protected from ring-opening to ketenimine **13**: on inclusion of zero-point energies, the transition state for this process fell below the energy of **14** from which we conclude that this azirine, once formed, decays spontaneously to **13**.

In contrast, the aromatic azirines **15** and **18** are solid minima, close to or slightly below the energies of the singlet naphthylnitrenes from which they are formed. It is gratifying to note that the two methods we used in the calculations predict quite similar reaction and activation energies for cyclization of the naphthylnitrenes to the azirines, although the restricted B3LYP wave function is unstable toward UHF at the transition state geometry (see Experimental Methods).

However, Karney and Borden found that CASPT2 has a tendency to overestimate the stability of open-shell singlet states of nitrenes as compared to (closed-shell) azirines and that this tendency may also lead to an overestimation of the barrier for cyclization (by ca. 3 kcal/mol in the case of the parent phenylnitrene).[22] If we assume that the same error carries over

Scheme 3. Energies of Valence Isomers of **1**[a]

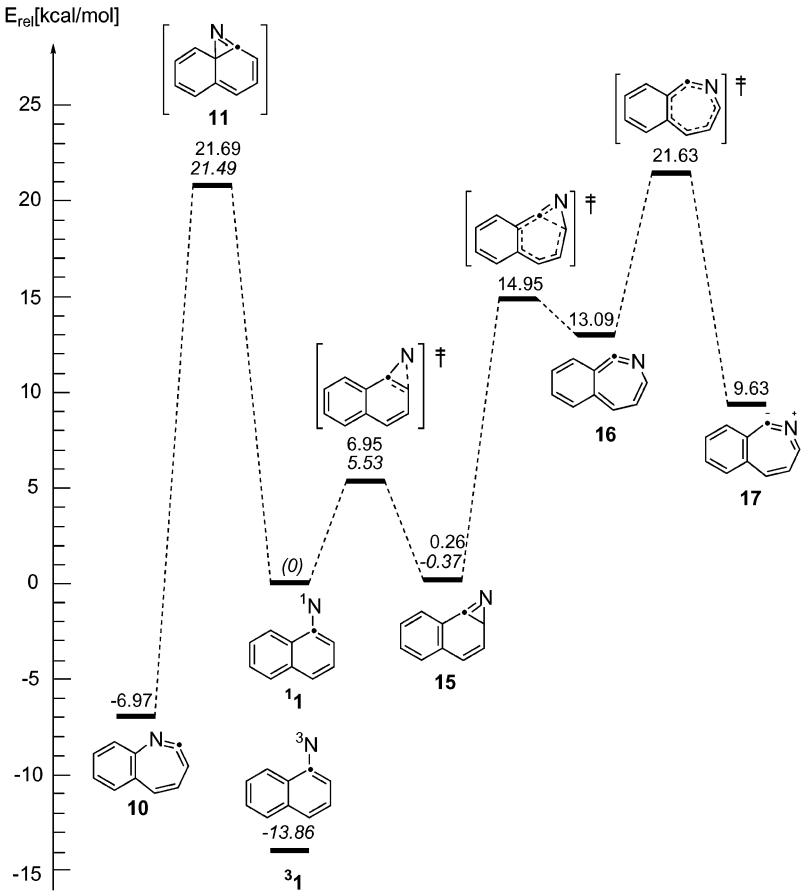

[a] Italic: CASPT2//CASSCF(12,12)/6-31G* energies relative to ^{1}**1**. Normal font: B3LYP/6-311+G(2d,p)//B3LYP/6-31G* energies relative to ^{3}**1** plus S/T gap from the above CASPT2 calculation. All energies include zero-point energy corrections at the level used for geometry optimization. Note that **11** is a transition state by DFT, but a (presumably shallow) minimum by CASSCF.

to the naphthylnitrene series (which may or may not be true), then the cyclization of ^{1}**2** would be nearly activationless, in contrast to the recently studied *o*-biphenyl-[32] or *o*-(di)alkylnitrenes[33] where activation barriers for cyclization to azirines of 6−9 kcal/mol were found.[46] If this is really the case, then intersystem crossing to ^{3}**2** would presumably be quenched by cyclization to **18**; that is, ^{3}**2** would have to be formed in a secondary process from **18** (or, eventually, **20**) in the above-described matrix experiment. As **20** (and presumably also **18**) absorbs at 313 nm, the wavelength used to deazotate azide **4**, this possibility cannot be excluded.

Because the ketenimines **16** and **19** that derive from the stable azirines **15** and **18** both have *o*-quinoid π-systems, it comes as no surprise that the ring expansion of these azirines is endothermic (cf. Schemes 3 and 4). In fact, the barriers for the reversion of these ketenimines to azirines are only 2−3 kcal/mol, so that ketenimines **16** and **19** are not expected to have significant lifetimes, even under cryogenic conditions. However, as in the case of the quinoyl nitrene systems discussed previously,[14] *o*-quinoid ketenimines such as **16** and **19** can recover an aromatic benzene ring by adopting zwitterionic (or carbenic) character, as in **17** and **20**. As it turns out, these structures are not resonance forms, but correspond to distinct potential energy minima with significantly different geometries (cf. Figure 10 below), which are separated by sizable barriers, although the C−C and C−H connectivities remain unchanged. In both cases, the formation of these ylidic forms of the heterocumulenes is a slightly exothermic process. However, once formed, these heterocumulenes are well protected from further decay, which explains why, in the photochemical experiments described above, these species rather than their metastable *o*-quinoid "bond-shift-isomers"[47] **16** and **19** were observed.

In sum, the calculations demonstrate that all observed species correspond to reasonably solid minima on the $C_{10}H_7N$ potential energy surface and that the species in Scheme 1 which were not observed (azirines **11** and **14**, and ketenimines **16** and **19**) are invariably close to low-lying transition states; that is, they are not expected to persist because they are not protected from decay to more stable isomers.

2.2. Excited States. 2.2.1. Naphthylnitrenes. To understand the nature of the electronic transitions of the triplet naphthylnitrenes, we ran TD-DFT and CASSCF/CASPT2 calculations on ^{3}**1** and ^{3}**2**, the results of which are shown in Table 1. Although the two methods do not agree quantitatively, they concur in predicting that in the case of ^{3}**1** the group of bands in the 400−600 nm range are comprised of *two* transitions, both involving excitations within the π system. We cannot assign individual

(46) The reason for the smaller activation energies for cyclization of naphthyl as compared to phenylnitrenes may be due to the fact that the naphthylnitrenes preserve an aromatic ring during this process, whereas the phenylnitrenes do not.

(47) For the concept of bond-shift isomers, see: Herges, R. *Angew. Chem., Int. Ed. Engl.* **1994**, *33*, 255 (Section 4.4.1).

Scheme 4. Energies of Valence Isomers of **2**[a]

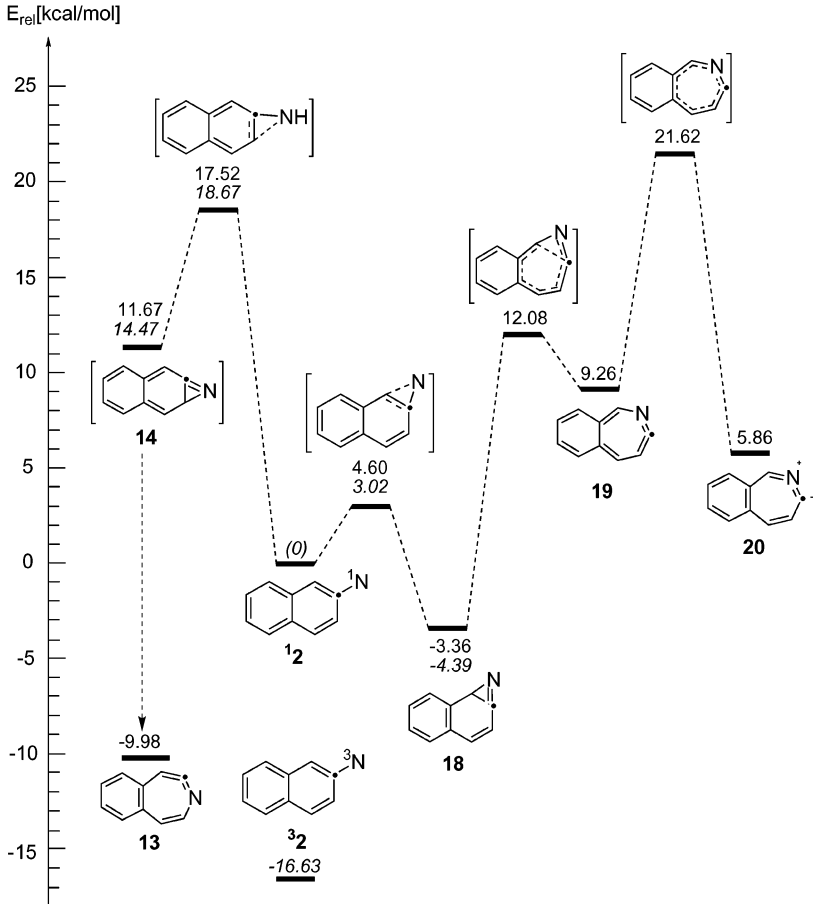

[a] Italic: CASPT2//CASSCF(12,12)/6-31G* energies relative to ^{1}**2**. Normal font: B3LYP/6-311+G(2d,p)//B3LYP/6-31G* energies relative to ^{3}**2** plus S/T gap from the above CASPT2 calculation. All energies include zero-point energy corrections at the level used for geometry optimization.

peaks in the spectrum of **1** to these two transitions, and such an undertaking may indeed be futile because the two states may be subjected to strong vibronic interaction, as they often are in compounds with close-lying electronic excited states.[48] The assignments for the first two transitions proposed in Table 1 should therefore be taken as tentative.

The spectrum of **2** shows a train of peaks between 450 and 600 nm that invites an interpretation in terms of a Franck−Condon envelope for a single electronic transition involving vibrational progressions of ca. 1360 and 350 cm^{-1}. Also, both theoretical methods predict a ca. 100 nm gap between the first two excited states which is more difficult to reconcile with an interpretation similar to that given above for **1**. Thus, we prefer to assign the second transition in **2** to the band at 427 nm, which brings it also into reasonably quantitative agreement with the calculations. It is also gratifying to note that the bathochromic shift of the first transition on going from **1** to **2** is reproduced by the calculations. However, a quantitative accord between experiment and prediction by the two methods is not achieved for the first two transitions.

In both naphthylnitrenes, the first two transitions are followed by more intense absorptions below 370 nm. For **1**, both methods predict a comparatively intense band at 351 or 340 nm, respectively, and one is tempted to assign this transition to the sharp band at 358 nm, followed perhaps by a vibrational progression of ca. 970 cm^{-1} at 346 nm, in the experimental spectrum. According to TD-B3LYP, this is followed by a weak band that may be difficult to discern and then by another intense transition at 309 nm which we assign to the band system peaking at 319 nm in the experimental spectrum.

The $7^3A''$ excited state predicted by the DFT calculations is interesting because it is unique to nitrenes: it involves promotion of a β-electron from the sp lone pair at the N atom (MO 33) to the singly occupied p_y-AO that is perpendicular to it (MO 38). This transition is predicted to occur at an energy similar to that in phenylnitrene,[49] which is not unexpected in view of its nature. However, the predicted oscillator strength for this transition is too weak to permit its location in the experimental spectrum (because the N lone pair was not included in the CASSCF active space, the corresponding transition could not be calculated by CASPT2. Instead, we list in Table 1 three additional weak $\pi \rightarrow \pi^*$ transitions predicted in this region by CASPT2).

In nitrene **2**, the situation with regard to the assignment of the UV bands is less clear, because the two methods disagree quite strongly, especially with regard to the transition moments. TD-B3LYP predicts two close-lying strong transitions around 350 nm, whereas CASSCF/CASPT2 predicts only a single transition of intensity similar to that of the first two in this

(48) See, for example, the case of the benzyl radical: Eiden, G. C.; Weisshaar, J. C. *J. Chem. Phys.* **1996**, *104*, 8896.

(49) Gritsan, N. P.; Zhu, Z.; Hadad, C. M.; Platz, M. S. *J. Am. Chem. Soc.* **1999**, *121*, 1202.

Table 1. Excited State Energies and Transition Moments of Naphthyl Nitrenes **1** and **2** by Calculations and Experiment

		TD-B3LYP[a]		CASSCF/CASPT2[b]		experiment	
		λ_{max} [nm]	$f \times 10^2$	λ_{max} [nm]	$f \times 10^2$	λ_{max} [nm][c]	excited state composition[d]
1	$2^3A''$	459	0.76	510	0.30	**535**/532/520	$36\beta \rightarrow 37\beta(0.87) + 38\alpha \rightarrow 39\alpha(0.56)$
	$3^3A''$	418	0.77	452	0.09	503/**496**/485 (?)	$35\beta \rightarrow 37\beta(0.93) + 38\alpha \rightarrow 40\alpha(0.40)$
	$4^3A''$	351	4.97	340	0.47	358(/346)	$38\alpha \rightarrow 39\alpha(0.69) + 36\beta \rightarrow 37\beta(0.43) +$ $36\beta \rightarrow 39\beta(0.39) + 37\alpha \rightarrow 39\alpha(0.29)$
	$5^3A''$	322	0.54	304	0.06	340 (?)	$34\beta \rightarrow 37\beta(0.50) + 36\beta \rightarrow 39\beta(0.48) +$ $37\alpha \rightarrow 39\alpha(0.46)$ + many others
	$6^3A''$	309	7.9	280	1.03	330/**319**/307	$38\alpha \rightarrow 40\alpha(0.82)$ + four others (each ~0.2)
	$7^3A''$	296	0.02	295−276[e]	small[e]		$33\beta \rightarrow 38\beta(0.93) + 30\beta \rightarrow 38\beta(0.30)$
	$1^3A'$	381	$<10^{-2}$	349	$<10^{-2}$		$36\beta \rightarrow 38\beta(0.87)$
2	$2^3A''$	507	0.93	535	0.27	**585**/574/561	$36\beta \rightarrow 37\beta(0.95) - 38\alpha \rightarrow 39\alpha(0.47)$
	$3^3A''$	393	0.51	415	0.33	**427**/414	$36\beta \rightarrow 39\beta(0.59) + 35\beta \rightarrow 37\beta(0.53) +$ $37\alpha \rightarrow 39\alpha(0.52) + 38\alpha \rightarrow 39\alpha(0.25) +$ ....
	$4^3A''$	354	2.34	353	0.27	(**354**/340)?	$35\beta \rightarrow 37\beta(0.71) - 37\alpha \rightarrow 39\alpha(0.52) +$ $36\beta \rightarrow 39\beta(0.39) + 38\alpha \rightarrow 40\alpha(0.36)$
	$5^3A''$	350	4.93	331	4.34	**354**/340	$38\alpha \rightarrow 39\alpha(0.47) - 37\alpha \rightarrow 39\alpha(0.26) +$ $36\beta \rightarrow 37\beta(0.26) + 36\beta \rightarrow 39\beta(0.25) +$ ....
	$6^3A''$	304	0.08	344	0.07		$34\beta \rightarrow 37\beta(0.84) + 38\alpha \rightarrow 41\alpha(0.41) +$ ...
	$7^3A''$	290	0.25	294−265[f]	small[f]		$33\beta \rightarrow 38\beta(0.97)$
	$1^3A'$	370	$<10^{-2}$	331	$<10^{-2}$		$36\beta \rightarrow 38\beta(0.96)$

[a] Based on B3LYP/6-31G* geometries. [b] CASPT2(12,12)/ANO-S based on CASSCF(12,12)/6-31G* geometries. [c] Bold: band maxima. [d] In the TD-B3LYP calculation; in terms of excitations within the manifold of MOs shown in Figures S2 (**1**) and S3 (**2**). Only the first $^3A'$ state is shown. [e] Three transitions with oscillator strengths between 0.07 and 0.1 at 295, 282, and 276 nm. [f] Three transitions with oscillator strengths between 0.008 and 0.15 at 294, 271, and 265 nm.

region, followed by a much weaker one further in the UV. The former prediction would seem to be in much better agreement with experiment, which shows an intense band peaking at 354 nm which could well be composed of two transitions.

The sp(N) → p_y(N) transition in **2** ($1^3A'' \rightarrow 7^3A''$) is predicted to occur at almost the same energy as in **1** but once more with a very small oscillator strength.

2.2.2. Ring Expansion Products. For the photoproducts of **1** and **2** (whose spectra are shown in Figures 1 and 5), attempts to run CASSCF/CASPT2 calculations did not result in a satisfactory description of the excited states for active spaces of computationally accessible size, so we contented ourselves with TD-DFT calculations on the first five excited states, the results of which are collected in Table 2.

With regard to the azirines **15** and **18**, these calculations predict a weak absorption around 320 nm (which is not observed as such, but must be present because these azirines can be photolyzed at 313 nm), followed by a stronger transition around 290 nm which must be responsible for the observed increase in absorption below 300 nm in spectrum 1f/1g. More transitions follow in the UV where we could not discern any bands due to strong absorptions of other products.

The broad bands of the novel ylidic heterocumulenes **17** and **20** are predicted to consist of two transitions, a weak one at ca. 495 nm and a stronger one at 468 nm in **17** and 435 nm in **20**, respectively. The predictions for the two strong transitions are in excellent accord with the observed λ_{max} of the broad bands, so we conclude that the first, weak transition must be hidden in the long wavelength tail of these bands which extends beyond 550 nm in both compounds. The two transitions are positive and negative linear combinations of the excitations from the HOMO of **17** and **20**, which is centered on the hypovalent carbon atom in both compounds (MO no. 37 in Figure 9) to the LUMO (no. 38) and the LUMO+1 (no. 39). A weak transition is predicted at ca. 300 nm, followed in the case of **17** by a stronger one at 285 nm, which would be in good accord with the band at 270 nm (cf. Figure 1h).

With regard to the "normal" ketenimines, **10** and **13**, the calculations predict strong bands at ca. 375 nm, that is, close to λ_{max} of the observed bands. As in the case of **17** and **20**, these transitions are linear combinations of HOMO → LUMO and HOMO → LUMO+1 excitations which involve MOs of the type shown for **10** in Figure 9. In contrast to the ylidic heterocumulenes, the negative combination of these two excitations (which gives rise to a weaker transition) is predicted to occur at higher energy than the positive one (which is responsible for the strong transition), presumably due to the effect of higher lying configurations which depress the latter state. In accord with our observations, no further strong bands are predicted to occur down to 250 nm.

Inspection of the MOs involved in the observed excitations (Figure 9) reveals a surprising similarity between the "normal" ketenimines **10** and **13** and the ylidic species **17** and **20**, respectively (only **10** and **17** are shown in Figure 9; the corresponding figure for **13** and **20**, which show very similar MOs, is found in the Supporting Information), with regard to both their structures and their one-electron wave functions. In both cases, the HOMO (no. 37) and the two lowest virtual MOs (nos. 38 and 39) are combinations of the lone pairs on the N and on the ylidic or cumulenic C atom (C1 in **17** and C2 in **10**) supplemented by some π contributions, whereas the HOMO−1 (no. 36) is largely located on the benzene ring. However, the MO energies and the configurational mixing are different (cf. Table 2); consequently the two classes of compounds absorb at different wavelengths.

2.3. The Geometric and Electronic Structure of Cyclic Ketenimine Isomers. The bicyclic ketenimines **10** and **13** have geometries that are very similar to that of the monocyclic ketenimine that is obtained by ring expansion of phenylnitrene[22] (Figure 10). A comparison with the unstrained, open-chain reference *N*-phenyl-*C*-vinylketenimine **29** (top of Figure 10) shows that the bond lengths in the cyclic RHC═C═NR′ moiety are within 0.01 Å of those in **29**, although this moiety is severely bent (ca. 155°), and that the dihedral angles are far from the

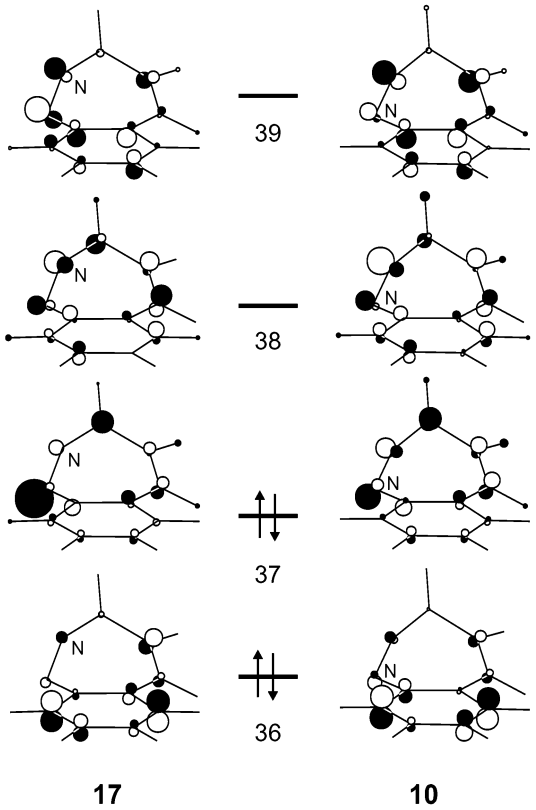

Figure 9. B3LYP molecular orbitals of **17** and **10** involved in the electronic transitions listed in Table 2. Similar MOs are obtained for **13** and **20** (cf. Supporting Information).

ideal 90° in **10** and **13**. Also, the bond lengths in the benzene ring all lie between 1.39 and 1.41 Å, indicating that this ring must be regarded as aromatic. The distortion of the ketenimine moiety in **10** and in **13** expresses itself in a lowering of the C═C═N stretching frequency (listed in parentheses in Figure 10) that corresponds to the most intense band in the IR spectrum by about 100 cm^{-1} relative to the comparable open-chain ketenimine **29**.

In contrast to the aromatic ketenimines **10** and **13**, the related *o*-quinoid ketenimines **16** and **19** show strongly alternating bond lengths (typically 1.44/1.36 Å) in the benzene ring and shortened C═C bonds exocyclic to that ring, in agreement with their *o*-quinoid valence structures. In these compounds, the calculated C═C═N stretching frequency is further lowered from that in **29**, possibly due to significant admixture of an iminocarbene valence structure which restores aromaticity in the benzene ring. However, as **16** and **19** are not observed, this prediction cannot be verified.

As we[14] and others[22] have found previously, formally zwitterionic (nitrile ylide) structures such as **17** and **20**, which at first sight might appear as resonance structures of **16** and **19**, have an existence all of their own in that they represent distinct energy minima separated by considerable barriers from their conventional ketenimine isomers, **16** and **19**. To understand the nature of these isomers which have common connectivities and differ only in their bond lengths and angles, we deemed it judicious to consider first the parent compounds, **30** and **31**, which had been investigated previously by Karney and Borden[22] using the CASSCF method (Scheme 5 and Table 3).

30 and **31**, whose geometries are similar to those of **17**/**20** and **16**/**19**, respectively (see Figure 10 and Table 3), also represent energy minima, separated by a barrier of about 10 kcal/mol, on the B3LYP/6-31G* potential energy surface. The two species reveal their pedigrees on planarization which yields the planar heteroannulenes **30′** and **31′**, respectively (Scheme 6), both of which are saddle points on the C_6H_5N potential energy surface. **30′** is a 6π aromatic system which is best represented by an azacycloheptatrienylidene resonance structure with lone pairs on adjacent C and N atoms, whereas **31′** is an 8π antiaromatic azacycloheptatetraene system with a vacant nonbonding in-plane AO on the central cumulenic C-atom. The electronic natures of the two species express themselves, for example, in the much more pronounced bond length alternation prevailing in **31′**, but also in the NICS values of the two species (Table 3) which are quite similar to those of benzene (−8.0) and planar cyclooctatetraene (+43.1), respectively. Thus, the claim of Karney and Borden that "cyclic delocalization is not

Table 2. Excited State Properties of Observed Naphthylnitrene Ring Expansion Products

compound	state no.	λ_{max}^{calc} [nm]	λ_{max}^{exp} [nm]	*f*	excited state composition[a]
15	1	317	(<320)	0.0131	37 → 39 (0.50) − 37 → 38 (0.42)
	2	292	<300	0.0460	37 → 39 (0.45) + 37 → 39 (0.37)
	3	264		0.0280	36 → 39 (0.48) + many others
	4	251		0.0582	36 → 38 (0.58) + 37 → 40 (0.20)
	5	238		0.0736	37 → 40 (0.49) + many others
10	1	373	355	0.0290	37 → 38 (0.60) + 37 → 39 (0.21)
	2	351		0.0074	37 → 39 (0.64) − 37 → 38 (0.23)
	3	272	(290)	0.0082	36 → 38 (0.63) + many others
	4	263		0.0021	36 → 39 (0.44) + many others
	5	256		0.0023	37 → 40 (0.50) − 35 → 38 (0.48)
17	1	494	(>470)	0.0050	37 → 38 (0.58) + 37 → 39 (0.34)
	2	468	470	0.0178	37 → 39 (0.57) − 37 → 38 (0.26)
	3	302		0.0110	37 → 40 (0.63) + 36 → 38 (0.21)
	4	285	270	0.0250	36 → 38 (0.59) − 36 → 39 (0.27)
	5	271		0.0018	35 → 38 (0.52) + 36 → 39 (0.42)
18	1	327	(<320)	0.0067	37 → 38 (0.63) + 36 → 38 (0.20)
	2	286	<300	0.0828	36 → 38 (0.53) − 37 → 39 (0.26)
	3	261		0.0187	(strongly mixed)
	4	253		0.0517	37 → 39 (0.46) − 35 → 38 (0.37)
	5	239		0.0248	(strongly mixed)
13	1	377	360	0.0295	37 → 38 (0.64) − 36 → 38 (0.12)
	2	334		0.0074	37 → 39 (0.66) − 36 → 38 (0.11)
	3	283		0.0300	36 → 38 (0.60) + 36 → 39 (0.26)
	4	268		0.0091	37 → 40 (0.51) − 36 → 39 (0.38)
	5	244		0.0441	35 → 38 (0.48) − 37 → 40 (0.39)
20	1	497	(>440)	0.0053	37 → 38 (0.67)
	2	435	440	0.0401	37 → 39 (0.60) + 37 → 40 (0.12)
	3	310		0.0070	37 → 40 (0.63) + 36 → 38 (0.24)
	4	278		0.0128	36 → 39 (0.62) + 36 → 38 (0.23)
	5	261		0.1173	36 → 38 (0.47) + 35 → 39 (0.36)

[a] In terms of excitations within the B3LYP/6-31G* MOs (no. 37 is the HOMO). The MOs of **17** and **10** are shown in Figure 9; those of the other compounds are given in the Supporting Information.

Scheme 5

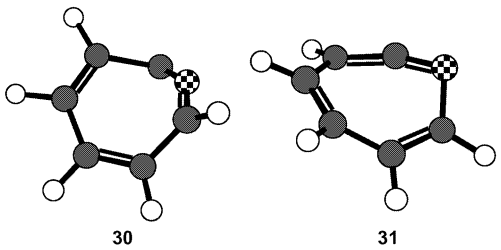

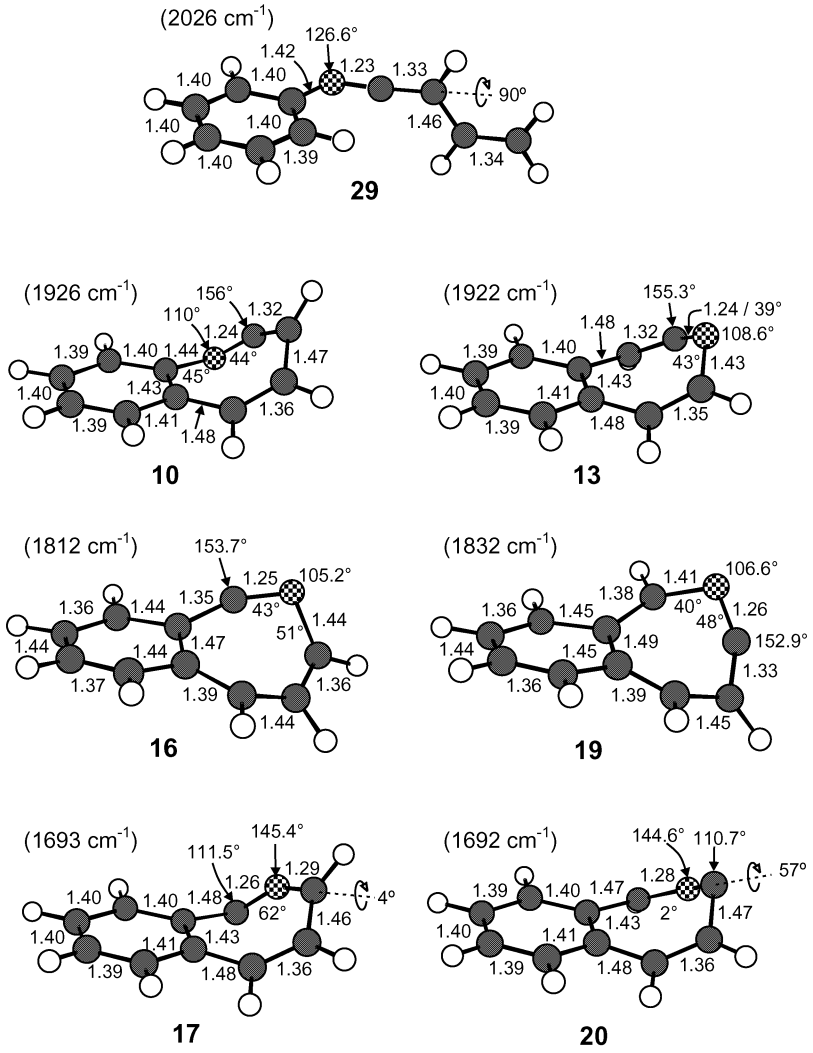

Figure 10. Bond lengths and some bond angles (next to atoms) and dihedral angles (next to bonds) of ketenimines. In parentheses: frequency of the C═C═N stretching vibration.

Scheme 6. Isodesmic Reactions Used To Assess the Factors that Stabilize or Destabilize **30** and **31**

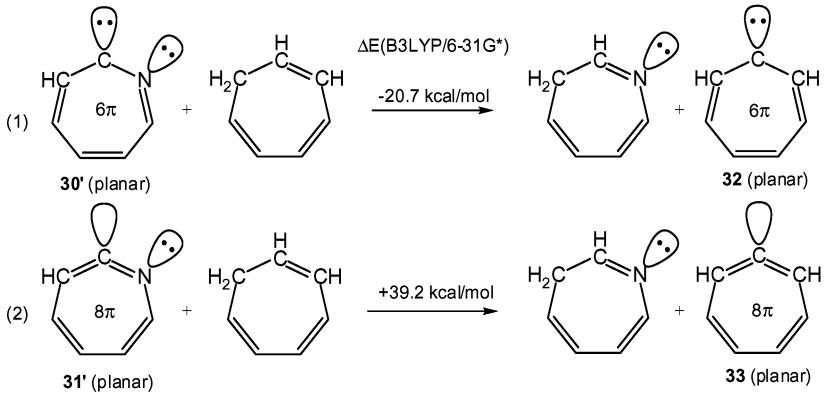

extensive" in **30′** (**^{1}A′-4a** in their paper) because it "requires transfer of π electrons to a neutral carbon" appears to be unfounded.

However, despite its aromaticity, planar **30′** lies 13.4 kcal/mol *higher* in energy than the antiaromatic planar **31′**, so some factor must offset the strong bias imposed by the cyclic delocalization of 6 versus 8 π-electrons. A hint is given by the length of the bond between the hypovalent C and the N atom which is almost as long in **30′** as the C(sp^2)−N═C single bond in **29** (1.40 vs 1.42 Å), despite its expected shortening due to cylic delocalization. Presumably, this is due to the repulsion between the lone pairs which are forced to be coplanar in **30′**. In contrast, the corresponding C═N bond in **31′** is even shorter than the N═C double bond in **29** (1.20 vs 1.23 Å), which may in turn be due to a bonding interaction between the N lone pair and the empty in-plane sp AO on the central cumulene C atom.

To estimate the energetic consequences of these factors, we calculated the isodesmic reactions shown in Scheme 6, which

Table 3. Geometrical Parameters, ChelpG Charges,[44] Relative Energies, and NICS Values[42] of Seven-Membered Ring Heterocycles at Their Equilibrium Geometries (**30** and **31**) and at the Optimized Planar Geometries (**30′** and **31′**)

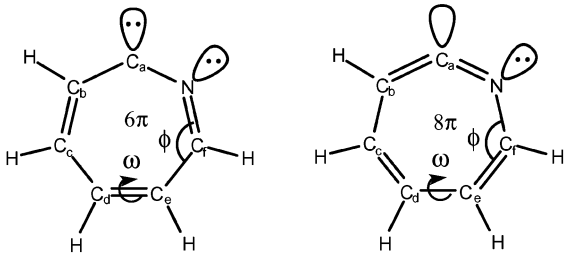

30 **31**

	30′ (C_s)		**30** (C_1)		**31′** (C_s)		**31** (C_1)	
	r [a]	ω [b]	r [a]	ω [b]	r [a]	ω [b]	r [a]	ω [b]
$N-C_a$	1.397	(0)	1.272	57.7	1.204	(0)	1.250	40.2
C_a-C_b	1.463	(0)	1.478	52.7	1.330	(0)	1.324	16.4
C_b-C_c	1.385	(0)	1.362	5.2	1.496	(0)	1.471	37.4
C_c-C_d	1.412	(0)	1.469	31.6	1.353	(0)	1.362	1.0
C_d-C_e	1.376	(0)	1.358	0.8	1.505	(0)	1.462	32.1
C_e-C_f	1.423	(0)	1.460	33.9	1.338	(0)	1.359	4.0
C_f-N	1.320	(0)	1.288	0.9	1.440	(0)	1.428	45.0
	q [c]	ϕ [d]	q [c]	ϕ [d]	q [c]	ϕ [d]	q [c]	ϕ [d]
N	−0.29	130.7	+0.04	145.5	−0.31	123.9	−0.41	107.2
C_a	−0.59	119.5	−0.39	108.0	+0.49	160.5	+0.31	155.6
C_b	+0.82	135.4	+0.34	118.3	−0.52	105.3	−0.30	109.2
C_c	−0.50	127.2	−0.35	128.4	+0.03	130.5	0.0	120.3
C_d	+0.28	126.1	+0.15	127.5	−0.19	130.7	−0.05	127.4
C_e	+0.14	127.4	−0.16	119.5	+0.03	129.3	−0.18	128.0
C_f	−0.11	133.7	+0.06	116.8	−0.05	119.9	+0.18	121.0
E_{rel} [e]	40.6		18.3		27.2		(0)	
NICS [f]	−9.31		−1.61		+36.4		+3.02	

[a] Bond length in Å. [b] Dihedral angle around bond in degrees. [c] CHelpG charge on heavy atom. [d] Bond angle at heavy atom in degrees (value in regular heptagon: 128.6°). [e] Relative energy in kcal/mol. [f] NICS value (cf: benzene, −8.0; planar cyclooctatetraene, +43.1).

allow a separation of the vicinal nonbonding in-plane AOs of **30′** and **31′** into two molecules while maintaining the aromatic or antiaromatic π electronic structure of the rings (note that planarity is also enforced in the product species **32** and **33**, but not in the azacycloheptatrienes which are taken at their equilibrium geometries). Thus, we found that reaction 1 is exothermic by 20.7 kcal/mol, whereas reaction 2 is endothermic by all of 39.2 kcal/mol. The first number is a measure of the lone pair repulsion which prevails in **30′**, while the second number measures the apparently quite considerable extra bonding interaction which involves the in-plane sp^x AOs in **31′**.

On relaxation from the planar geometry, **30′** undergoes a 57.7° twisting around the $N-C_a$ bond (ω in Table 3). The concomitant attenuation of the lone pair repulsion is achieved at the expense of an almost complete loss of the aromaticity that prevails in **30′** (the NICS value increases to −1.6). On the basis of reaction 1 in Scheme 6, we estimate that these two factors nearly cancel in energy, so the net stabilization of 22.3 kcal/mol in **30** (at its nonplanar equilibrium geometry) must be due to an additional factor. Indeed, the spectacular shortening (−0.125 Å) that accompanies the twisting of the C−N bond indicates that some extra bonding must be gained in the process. The origin of this bonding can be traced by allowing the twisting to proceed to 90°, which brings the N lone pair into coplanarity with the empty p-AO on the formerly carbenic C atom in **30′**, thus allowing the formation of a new π-bond in **30** (cf. Scheme 7).

Scheme 7. Iminocarbenes versus Nitrile Ylides

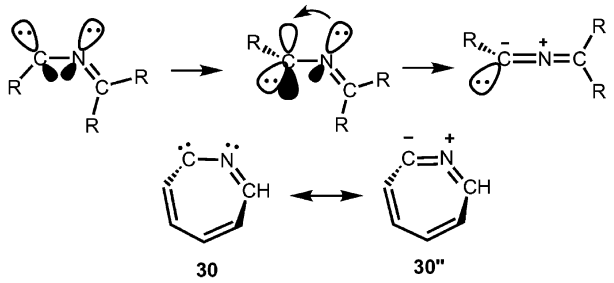

30 **30"**

The strength of this π-bond is maximized when the C−N−C moiety becomes linear; that is, the former iminocarbene assumes the structure of a nitrile ylid.[50] While the constraints imposed by the seven-membered ring structure of **30** do not allow this structure (**30″** in Scheme 7) to be fully realized, the C−N−C angle does open up to 145.5°, and the C_a-N and the $N-C_f$ bond lengths in **30** (1.27 and 1.29 Å, respectively) are not far from those calculated previously for unconstrained nitrile ylides (ca. 1.22 and 1.28 Å, respectively).[51] Thus, **30** is better represented by a nitrile ylide **30″** than by an iminocarbene resonance structure **30**, although the high electronegativity of N prevents much positive charge from building up on that atom (cf. ChelpG charges in Table 3).

On relaxation of the planar ketenimine **31′**, the twisting around the $N-C_a$ bond proceeds only to 40.2°, thus maintaining part of the interaction between the formally nonbonding sp^x AOs (the C_a-N bond length increases only by 0.046 Å). On the other hand, much of the antiaromatic destabilization is lost by the pronounced twisting around the essential single bonds (the bond length alternation decreases significantly, and the NICS value drops to less than 10% of its value in **31′**), which allows **31** to reap much of the benefit from angular strain release. Hence, the stabilization realized on relaxing from the planar structure amounts to 27.2 kcal/mol in this case, which creates a net bias of 18.3 kcal/mol in favor of the (nonplanar) ketenimine structure **31** over the iminocarbene/nitrile ylide structure **30**/**30″**.

In the pairs **16**/**17** and **19**/**20**, the bias favoring the ketenimine structure **31** is reversed by the gain in resonance energy on going to the benzenoid structures **17** and **20**, which are each 3.4 kcal/mol more stable than the isomeric *o*-quinoid keteninimines **16** and **19**, respectively (Schemes 3 and 4).

This raises the question of why seemingly modest structural changes can give rise to such high barriers. An answer to this question can be found in a MO correlation diagram (Figure 11), which shows that the HOMO of the (observed) ylidic heterocumulene **17** correlates with a virtual MO of its *o*-quinoid relative, **16**, and vice versa (a similar correlation is found for the pair **19**/**20**). Hence, the ground states of the ylidic heterocumulenes correlate with doubly excited states of their bond-shift isomers,[47] the *o*-quinoid ketenimines, and vice versa, the signature of symmetry forbidden reactions (the present compounds have no symmetry, so the selection rules are not rigorous).

(50) Note that nitrile ylides, although derived from (linear) nitriles RCN: and singlet carbenes $:CR_2'$, do not usually retain a linear $R-C-N-CR_2'$ structure, but undergo R−C−N bending to assume a more stable allenyl anion type structure with an sp^2 lone pair at the C atom and perpendicular R−C−N and $N-CR_2'$ moieties (cf. Caramella, P.; Houk, K. N. *J. Am. Chem. Soc.* **1976**, *98*, 6397).

(51) Hegarty, A. F.; Nguyen, M. T. *J. Chem. Soc., Perkin Trans. 2* **2001**, 1239.

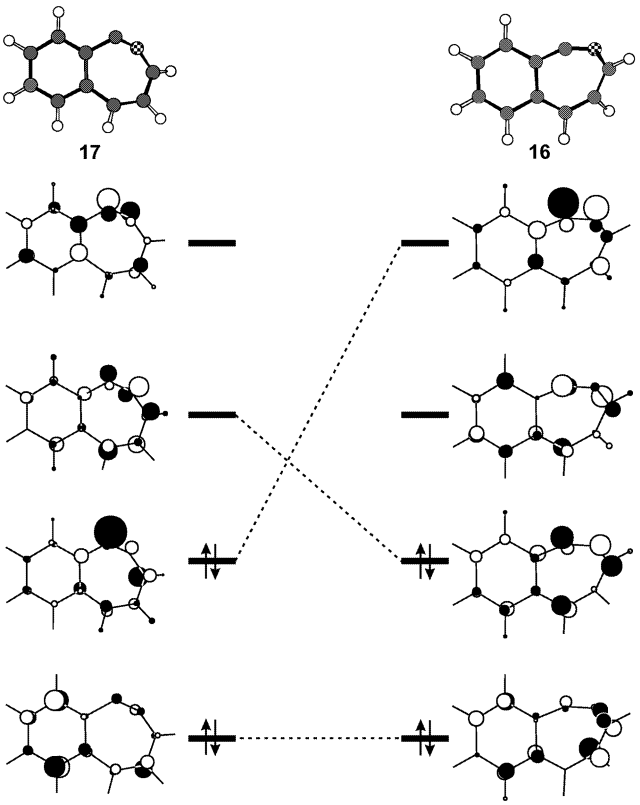

Figure 11. Orbital correlation diagram between **16** and **17**. For a discussion, see text.

Scheme 8

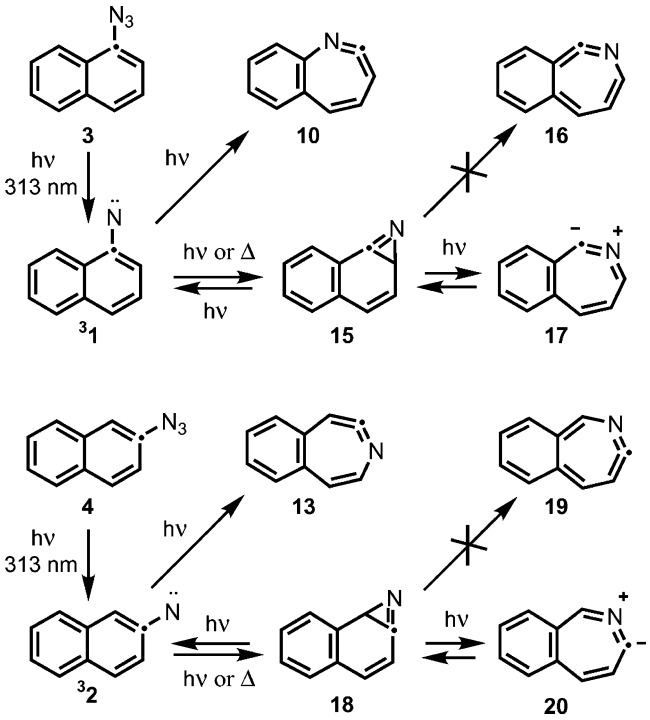

3. Conclusions

Scheme 8 summarizes the experimental observations made in the course of the present study. Thus, photolysis of 1- and 2-naphthyl azides **3** and **4** in an Ar matrix at 313 nm affords the corresponding triplet naphthylnitrenes, ^{3}**1** and ^{3}**2**, which are accompanied by the azirines **15**/**18** and the novel cyclic nitrile ylides **17**/**20**. These three types of compounds can be interconverted by irradiations at selected wavelengths. On continued irradiation at 313 nm, the seven-membered cyclic ketenimines **10** and **13**, respectively, begin to appear, whereby ketenimine **10** is accompanied by several byproducts which are thought to result from ring-opening reactions. The existence of ylidic heterocumulenes such as **17** and **20** has been predicted previously,[14] but this work provides their first experimental observation. The *o*-quinoid ketenimines **16** and **19**, which would constitute the "classical" ring-opening products of azirines **15** and **18**, respectively, are not observed. DFT calculations suggest that, if they were formed photochemically, they would thermally recyclize to the precursor azirines over very low barriers.

Despite the fact that ketenimines **16** and **19** are *o*-quinoid species while the cyclic nitrile ylides **17** and **20** profit from benzenoid resonance energy, the latter are only ca. 3.5 kcal/mol more stable than the former according to DFT calculations. This apparent lack of significant aromatic stabilization is due to an inherent energetic bias for the ketenimine over the cyclic nitrile ylide structure. This bias is barely counterbalanced by the gain in benzene resonance energy. The interconversions of the "bond-shift isomers" **16** and **17** (or **19** and **20**) involve fairly substantial barriers which arise by virtue of the fact that the pairs of compounds are "lumomers"; that is, their ground states correlate with doubly excited states of the respective products.

We attempted to characterize the electronic structure of the naphthylnitrenes **1** and **2** by CASSCF/CASPT2 and by TD-DFT calculations. These calculations permit a rather unambiguous assignment of the visible transitions, albeit with less than satisfactory quantitative agreement between calculated and observed band positions and intensities. In the UV region, the two methods yield partially contradictory predictions, and a reliable assignment is not possible.

Acknowledgment. This work was supported by the Swiss National Science Foundation (project No. 2000-067881.02), the Australian Research Council. and the U.S. National Science Foundation (grant CHE-0237256).

Supporting Information Available: Cartesian coordinates and absolute energies (including zero-point corrections) of all stationary points discussed in this study, and lists of calculated and observed IR frequencies of compounds ^{3}**1**, ^{3}**2**, **10**, **13**, **15**, **17**, **18**, and **20**. Molecular orbitals of **13** and **20** and IR spectrum of ketenimine **10** (PDF). This material is available free of charge via the Internet at http://pubs.acs.org.

JA038458Z